02

Luminescence of erbium ions in scandium-yttrium oxide ceramics

© A.V. Spirina[1], V.I. Solomonov[1], A.S. Makarova[1], V.V. Osipov[1], V.A. Shitov[1], R.N. Maksimov[1,2]

[1] Institute of Electrophysics, Ural Branch, Russian Academy of Sciences, Yekaterinburg, Russia
[2] Ural Federal University after the first President of Russia B.N. Yeltsin, Yekaterinburg, Russia

e-mail: rasuleva@iep.uran.ru

Received April 08, 2024
Revised September 13, 2024
Accepted January 09, 2025

The paper presents the research results of the luminescence of transparent mixed ceramics samples with the composition $Er_y:(Sc_xY_{1-x})_2O_3 + 2$ mol.% ZrO_2 at different scandium contents. Excitation of samples by laser diode radiation with a wavelength of 808 nm leads to up-conversion, as a result of which photoluminescence bands at the $^4S_{3/2} \rightarrow {}^4I_{15/2}$ (530–575 nm) and $^4I_{11/2} \rightarrow {}^4I_{15/2}$ (950–1050 nm) transitions appear in the visible and near IR regions of the spectrum. When excited by an electron beam with a duration of 2 ns with an average electron energy of 170 keV and a current density of 130 A/cm^2, along with yellow-green luminescence, there are additional emission bands of erbium ions, corresponding to the $^4F_{9/2} \rightarrow {}^4I_{15/2}$ (640–720 nm) and $^4S_{3/2} \rightarrow {}^4I_{13/2}$ (840–900 nm) transitions. With increasing scandium content in the samples, a red shift and broadening of the long-wavelength components of all erbium luminescence bands are observed. Using kinetic measurements, the lifetimes of the observed emissive levels have been determined.

Keywords pulsed cathodoluminescence, lifetime, up-conversion, erbium.

DOI: 10.61011/EOS.2025.01.60561.6219-24

Introduction

Solid-state lasers generating radiation in the mid-infrared (IR) range (1.5–2.1 μm) are of great interest for practical applications in communication lines, medicine, lidar devices, and etc. Crystals, glasses, and ceramic materials, in particular, doped with erbium ions, are used as the active media of such lasers (Er^{3+}). So far many oxide and fluorine materials have been known, such as $Y_3Al_5O_{12}$, $YAlO_3$, YVO_4, $GdVO_4$, $KGd(WO_4)_2$, $LiYF_4$, CaF_2 and other, doped with Er^{3+}, where at transitions $^4I_{11/2} \rightarrow {}^4I_{13/2}$ (2.5–3.1 μm) and $^4I_{13/2} \rightarrow {}^4I_{15/2}$ (1.5–1.6 μm) laser generation was obtained [1–5].

Promising materials for creation of near- and mid-IR region solid-state lasers, as well as devices using up-conversion radiation, are oxides Y_2O_3, Lu_2O_3 and Sc_2O_3activated by rare earth elements [6,7]. These substances have higher thermomechanical properties than garnet structure materials, which is an essential advantage [8,9], but at the same time it is difficult to grow such single crystals. Ceramic technology can significantly reduce the synthesis temperature (usually to 1700–1800 °C) and provides production scalability and simplifies the manufacture of highly doped materials of a specified composition and uniform distribution of doping impurities, which is necessary to create commercially available lasers. Therefore, the laser ceramics based on Y_2O_3, Lu_2O_3 and Sc_2O_3 oxides activated by rare-earth ions is currently being widely investigated [8,9].

Of special interest is transparent ceramics with its structure formed by solid solutions based on mixed oxides Y_2O_3–Lu_2O_3–Sc_2O_3. In this series, we may observe higher strength of crystal fields in the positions of rare-earth ions replacing oxide cations, which results in dependence of their Stark splitting on composition of the mixture [10]. In recent years, a transparent ceramics $(Lu_xSc_{1-x})_2O_3$, $(Lu_xY_{1-x})_2O_3$, doped with rare-earth ions of Yb^{3+} [11–13], Tm^{3+} [14–16] and Ho^{3+} have been obtained [17]. It has been shown that rare earth ions emit wide bands in mixed oxide ceramics, which make it possible to obtain short laser pulses [18,19].

The paper [20] outlines the technology and characteristics of transparent ceramics based on scandium and yttrium oxides mixed in different proportions and activated by Er^{3+}. Also this paper describes the study of photoluminescence behavior at laser transition $^4I_{11/2} \rightarrow {}^4I_{13/2}$ (2.55–3.1 μm) of erbium ion. It is shown that in this region the spectrum is represented by a wide-patterned band with a maximum at 2.716 μm and a long-wavelength band with a less intense width. With an increase in the scandium content, there is a broadening (from 22 to 34 nm) of the components of both bands, as well as a red shift of the maximum of the long-wavelength emission band from 2.842 to 2.848 μm.

The purpose of this study is to further investigate the spectral luminescent properties of these ceramics, but only in the visible and near-infrared regions when excited by a laser diode with a wavelength of 808 nm and a pulsed electron beam.

Objects of the study

In this study they used transparent ceramics samples $Er_y:(Sc_xY_{1-x})_2O_3 + 2$ mol.% ZrO_2 as discs 12 mm in diameter and 1.8 mm thick. Their characteristics are given in the Table 1.

Table 1. Characteristics of the studied objects $Er_y:(Sc_xY_{1-x})_2O_3 + 2$ mol.% ZrO_2

Sample	y	x	Lattice constant a, nm
1	0.075	0	1.05947
2	0.074	0.114	1.05067
3	0.073	0.227	1.04211
4	0.072	0.445	1.02521

Ceramics was sintered at a temperature of 1750 °C for 5 h in vacuum of 10^{-5} mbar in the high-temperature furnace with graphite heaters. The resulting discs were subjected to antireflection annealing in the air at a temperature of 1400 °C for 2 h, and then polished on both sides to a mirror-like shine. A small amount of (2 mol.%) zirconium dioxide (ZrO_2) was used as a sintering additive.

The crystalline phase of all ceramic samples is represented by a single-phase solid solution with a cubic bixbyite structure (*C*-type, sp. gr. *Ia*-3). No second phases, including those associated with the presence of ZrO_2, were discovered. With an increase in the scandium content in the samples, the crystal lattice constant (Table. 1) decreased in accordance with Vegard law. More detailed characteristics and ceramic samples fabrication technology are presented in [20].

Equipment

Transmission spectra were recorded on Shimadzu UV-1700 spectrophotometer in the range of 200–1100 nm with a scanning step of 1 nm.

Photoluminescence (PL) was excited by a laser diode (808 nm) with a power of 4 W and emission density not exceeding 0.5 W/mm^2 at room temperature of the samples and was recorded using a spectrometric complex based on MDR-41 monochromator, as well as a FEU-100 and FEU-62. The error of wavelength measurement didn't exceed 0.5 nm.

Pulsed cathodoluminescence (PCL) was excited using an electron accelerator that generated a beam with an average energy of 170 keV, current density of A/cm^2, with a duration of 2 ns at a repetition rate of 1 Hz. The samples were not subjected to diaphragmation; they were irradiated in the air at room temperature. The integral luminescence spectrum was recorded by a multichannel photodetector based on a CCD ruler in the range of 400–900 nm in one frame (exposure was 50 ms) and averaged over 60 pulses, which ensured the stability of the amplitude parameters of the spectrum no worse than 90 %. Diameter of the electron beam cross-section did not change during irradiation. Absolute error of wavelength measurement was ±0.3 nm. The spectral sensitivity was adjusted using AvaLigth -HAL-CAL (350–1100 nm) halogen calibration light source.

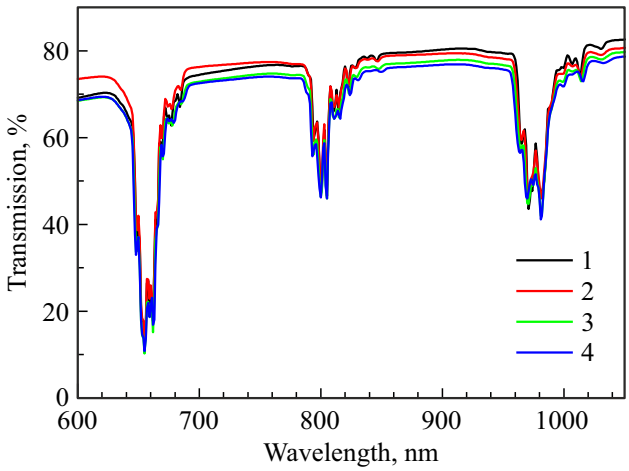

Figure 1. Transmission spectra of samples without addition of scandium and with its different contents. In the legends the sample numbers are indicated as per Table 1.

Table 2. Position of wavelengths in the samples' transmission band $Er_y:(Sc_xY_{1-x})_2O_3 + 2$ mol.% ZrO_2 depending on scandium content

Sample	x	Wavelength, nm				
		$^4I_{15/2} \rightarrow {}^4F_{9/2}$		$^4I_{15/2} \rightarrow {}^4I_{9/2}$	$^4I_{15/2} \rightarrow {}^4I_{11/2}$	
1	0	677	684	846	1013	1031
2	0.114	677	685	847	1014	1031
3	0.227	678	685	848	1014	1031
4	0.445	679	687	850	1016	1034

When measuring kinetic characteristics, the same excitation source was used, but MDR-41, FEU-100 and FEU-62 monochromators were used as receiving equipment, the signals from which were detected by Keysight DSOX2014A oscilloscope.

Results

Fig. 1 illustrates the transmission spectra in the region of 600–1050 nm. Three patterned absorption bands correspond to the electrons transition from the bottom level $^4I_{15/2}$ to the upper levels $^4F_{9/2}$, $^4I_{9/2}$, $^4I_{11/2}$ of Er^{3+} ion. In each band, most of the lines do not change their position with higher scandium content, except for the low-intensity lines located on the long-wavelength sides of each band. Table 2 shows the wavelengths that change their position with increase of the scandium content.

When samples are placed under the radiation of a laser diode with a wavelength of 808 nm, visually red transparent samples emit a yellow-green glow, the saturation of which decreases with an increase in the scandium content in the samples. In PL spectrum of all samples two patterned bands are detected at transitions $^4S_{3/2} \rightarrow {}^4I_{15/2}$ (530–575 nm) and $^4I_{11/2} \rightarrow {}^4I_{15/2}$ (950–1050 nm), and only in sam-

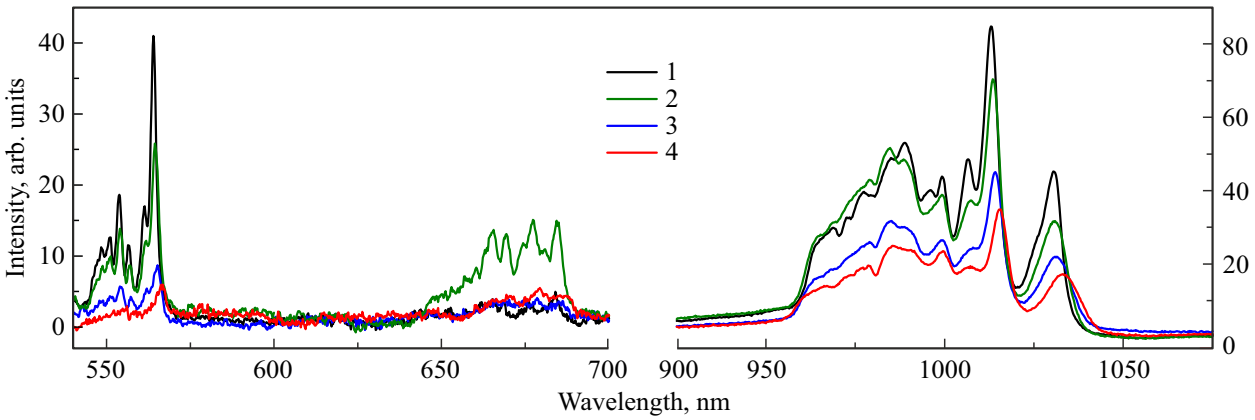

Figure 2. Photoluminescence spectra of samples In the legends the sample numbers are indicated as per Table 1.

ple № 2, apart from these bands, the red luminescence (640–690 nm) occurs at transition $^4F_{9/2} \rightarrow {}^4I_{15/2}$, hardly distinguished in other samples (Fig. 2).

With higher scandium content for all lines in the near-infrared band at 950–1050 nm, a shift of maxima from 1.2 to 2.8 nm to the long-wavelength region is observed (Fig. 2). This shift occurs due to an increase in the crystalline field at the positions of Er^{3+} ion, which is confirmed by lower value of lattice constant and increased scandium content in samples (Table. 1), and to which the lower multiplets of the ion energy levels are most sensitive. The upper multiplets, as shown by the transmission spectrum, practically do not change. There are no superlattice lines in the diffraction patterns, which indicates a disordered crystal structure of solid solutions, which leads not only to a shift, but also to a broadening of the luminescence bands with an increase in the scandium content. This is most clearly manifested in the IR-spectrum of PL (Fig. 2) for the long-wavelength line: in scandium-free samples ($\lambda = 1030.5$ nm) the line width is 8 nm, and in samples with the highest scandium content ($\lambda = 1033.3$ nm) this width rises up to 11 nm.

Given the results obtained, a circuit for energy levels excitation by a laser diode and the corresponding radiation were simulated (Fig. 3). Under photo-excitation of level $^4I_{9/2}$ some part of energy „goes“ to level $^4I_{11/2}$ without any radiation, and from this level the ground state transforms into radiative transition $^4I_{11/2} \rightarrow {}^4I_{15/2}$ with luminescence appearing in the region of 950–1050 nm (Fig. 2). From the same level $^4I_{11/2}$, the same exciting emission pumps a higher level $^4F_{7/2}$ (up-conversion), which is non-radiatively discharged to a lower level $^4S_{3/2}$ with the appearance of a yellow-green luminescence band at the transition $^4S_{3/2} \rightarrow {}^4I_{15/2}$. And only sample № 2 is distinguished by additional red luminescence at transition $^4F_{9/2} \rightarrow {}^4I_{15/2}$, where the upper level is excited as a result of non-radiative energy transfer from level $^4S_{3/2}$ (Fig. 3).

Fig. 4 shows the PCL spectra in the range of 520–900 nm. The infrared band (950–1050 nm) of the transition $^4I_{11/2} \rightarrow {}^4I_{15/2}$ is not registered in PCL spectrum due to the limitation of the spectral range of the integrating photodetector.

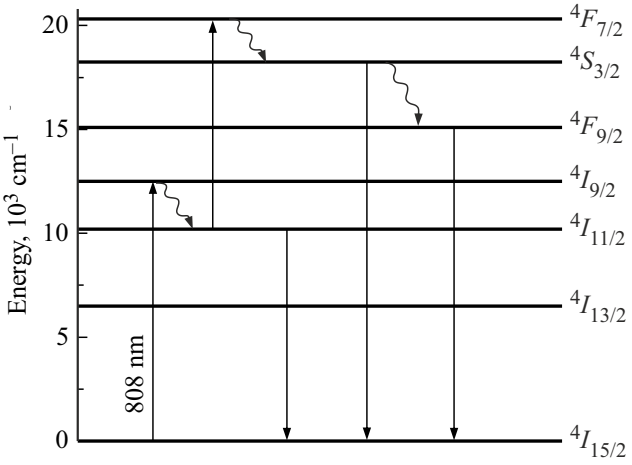

Figure 3. Scheme of excitation of energy levels and radiation Er^{3+} when exposed to a laser diode with a wavelength of 808 nm.

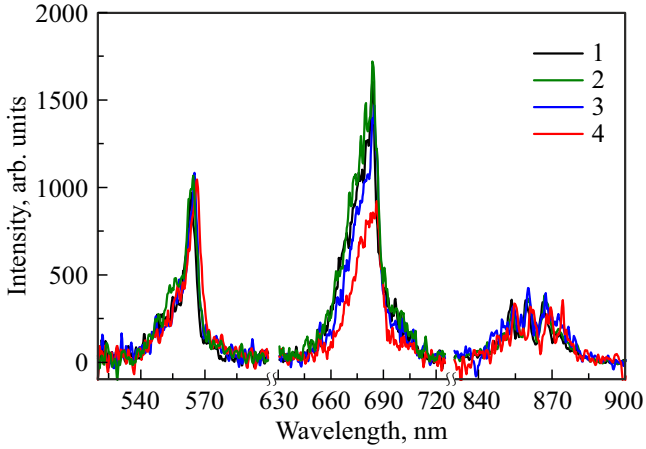

Figure 4. PCL spectrum of samples with different contents of scandium. In the legends the sample numbers are indicated as per Table 1.

Table 3. Position of the wavelengths in the luminescence spectrum of samples № 1 and № 4

Sample	Wavelength, nm				
	$^4S_{3/2} \rightarrow {}^4I_{15/2}$	$^4F_{9/2} \rightarrow {}^4I_{15/2}$	$^4S_{3/2} \rightarrow {}^4I_{13/2}$		
1	563.6	683.7	853.5	859.3	866.2
4	566.4	685.9	854.7	861.1	868.0

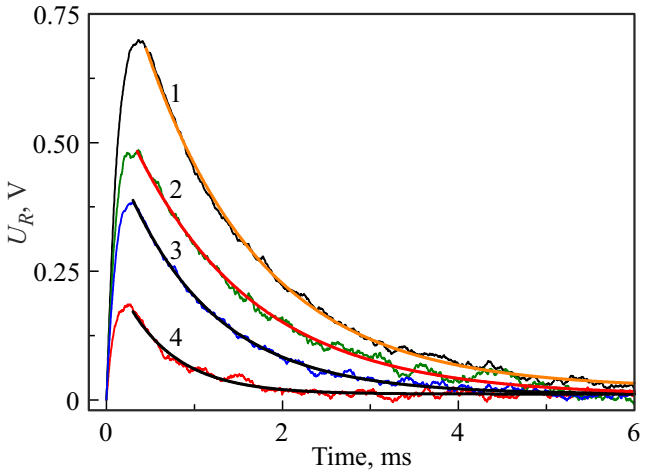

Figure 5. Kinetic dependences in maxima of PLC IR-band, measured at wavelengths 1030.5−1033.3 nm depending on the scandium content, and their approximation. The numbers next to curves correspond to the numbers of samples according to the Table 1.

Three patterned bands appear in PCL spectrum. As the scandium content increases, the maxima of the long-wavelength components of each PCL band, as well as during photo-excitation, are shifted from 1.2 to 2.8 nm into the long-wavelength region (Table 3). A distinctive feature of the spectra when excited by an electron beam (Fig. 4) and PCL (Fig. 2) is that in PCL for all samples with different scandium contents, a red band is observed at the transition $^4F_{9/2} \rightarrow {}^4I_{15/2}$ (640 −720 nm) and additional low-field occurs in the near-infrared region (840−900 nm) presumably at the transition $^4S_{3/2} \rightarrow {}^4I_{13/2}$ of erbium ion. This difference is due to the greater excitation efficiency of $^4S_{3/2}$ and $^4F_{9/2}$ levels by an electron beam relative to their excitation due to up-conversion by radiation from a 808 nm diode laser.

In almost all samples, when excited by an electron beam, the kinetics of the observed bands and their components are described by an exponential decrease in intensity with a characteristic time equal to the lifetime of the radiative transition level. For example, Figure 5 shows the time dependences for the most intense line observed in IR band of the photo-luminescence (Fig. 2). The intensity decay times for the bands at the transitions $^4S_{3/2} \rightarrow {}^4I_{15/2}$ and $^4S_{3/2} \rightarrow {}^4I_{13/2}$ inside the samples of the same composition turned out to be equal, which additionally indicates the emission of these bands from the general level $^4S_{3/2}$. In turn, the characteristic decay times of each band in samples of different compositions are noticeably different. (Table 4).

Table 4. Characteristic lifetime of levels for samples $Er_y:(Sc_xY_{1-x})_2O_3 + 2$ mol.% ZrO_2

Sample	x	Lifetime of level		
		$^4S_{3/2}$, μs	$^4F_{9/2}$, μs	$^4I_{11/2}$, ms
1	0	5.6	21.8	1.5
2	0.114	4.5	17.5	1.7
3	0.227	4.0	12.6	1.2
4	0.445	3.4	8.3	0.7

It can be seen that the lifetime of the radiative level $^4F_{9/2}$ decreases monotonously with an increase in the scandium content in the samples. Such drop in the lifetime is also observed for the level $^4S_{3/2}$, while for the radiative level $^4I_{11/2}$ the lifetime behavior is somewhat extreme in nature: for the scandium-free sample it makes 1.5 ms, in samples № 2 it increased to 1.7 ms, and further with higher scandium content the lifetime subsided to 0.7 ms. Let's bear in mind that during photo-excitation, a red luminescence band was observed only in samples of the same composition № 2, and in the rest sample it was practically not manifested. The reason for this behavior is not entirely clear and requires additional research, including fabrication of ceramics of intermediate compositions.

Conclusion

When level $^4I_{9/2}$ of the erbium ion is excited by a 808 nm wavelength laser diode the up-conversion is observed in all samples; this results in appearance of radiative bands at transitions $^4S_{3/2} \rightarrow {}^4I_{15/2}$ and $^4I_{11/2} \rightarrow {}^4I_{15/2}$, while samples № 2 additionally have radiation at transition $^4F_{9/2} \rightarrow {}^4I_{15/2}$. When excited by a pulsed electron beam, the same radiation bands are detected corresponding to the transitions similar as during photo-excitation. $^4S_{3/2} \rightarrow {}^4I_{15/2}$ (530−575 nm), $^4F_{9/2} \rightarrow {}^4I_{15/2}$ (640−720 nm), as well as band $^4S_{3/2} \rightarrow {}^4I_{13/2}$ (840−900 nm) which is absent in the PL. As the scandium content increases, a red shift and broadening of the long-wavelength components of all erbium luminescence bands are observed. Kinetic measurements have shown that the samples of composition № 2 have the longest lifetime of level $^4I_{11/2}$, which is 1.7 ms. The radiative levels $^4S_{3/2}$ and $^4F_{9/2}$ have lifetimes of the order of units and tens of microseconds and decrease with the scandium content growth in the samples.

Funding

This study was carried out under state assignment of the Ministry of Science and Higher Education of the Russian Federation (№ 124022200004-5).

Conflict of interest

The authors declare no conflict of interest.

References

[1] H. Strange, K. Petermann, G. Huber, E.W. Duczynski. Appl. Phys. B, **49**, 269 (1989). DOI: 10.1007/BF00714646
[2] X.F. Yang, D.Y. Shen, T. Zhao, H. Chen, J. Zhou, J. Li, H.M. Kou, Y.B. Pan. Laser Physics, **21** (6), 1013 (2011). DOI: 10.1134/S1054660X1111034X
[3] C. Brandt, V. Matrosov, K. Petermann, G. Huber. Opt. Lett., **36** (7), 1188 (2011). DOI: 10.1364/OL.36.001188
[4] D.Yu. Sachkov. Nauch.-Tekhn. vestnik SPbGU inf. tekhn. mekh. opt., **10** (1), 27 (2010) (in Russian).
[5] M.A. Noginov, V.A. Smirnov, A.F. Umyskov, G. Huber, H. Stange, I.A. Shcherbakov. Sov. J. Quant. Electron., **20** (10), 1185 (1990). DOI: 10.1070/QE1990v020n10ABEH007438.
[6] L. Fornasiero, E. Mix, V. Peters, K. Petermann, G. Huber. Cryst. Res. Technol., **34** (2), 255 (1999). DOI: 10.1002/(SICI)1521-4079(199902)34:2¡255::AID-CRAT255¿3.0.CO;2-U
[7] K. Petermann, G. Huber, L. Fornasiero, S. Kuch, E. Mix, V. Peters, S.A. Basun. J. Lumin., **87** (89), 973 (2000). DOI: 10.1016/S0022-2313(99)00497-4
[8] Ph.H. Klein, W.J. Croft. J. Appl. Phys., **38** (4), 1603 (1967). DOI: 10.1063/1.1709730
[9] A.A. Kaminskii, M.S. Akchurin, R. Gainutdinov, K. Takaichi, A. Shirakawa, H. Yagi, T. Yanagitani, K. Ueda. Crystallogr. Rep., **50** (5), 869 (2005).
[10] P. Loiko, P. Koopmann, X. Mateos, J.M. Serres, V. Jambunathan, A. Lucianetti, T. Mocek, M. Aguiló, F. Díaz, U. Griebner, V. Petrov, C. Krankel. IEEE J. Sel. Top. Quant. Electron., **24** (5), 1600713 (2018). DOI: 10.1109/JSTQE.2018.2789886
[11] W. Liu, H. Kou, J. Li, B. Jiang, Y. Pan. Ceram. Int., **41** (5), 6335 (2015). DOI: 10.1016/j.ceramint.2015.01.063
[12] G. Toci, A. Pirri, B. Patrizi, R.N. Maksimov, V.V. Osipov, V.A. Shitov, M. Vannini. J. Alloys Compd., **853**, 156943 (2020). DOI: 10.1016/j.jallcom.2020.156943
[13] W. Jing, P. Loiko, L. Basyrova, Y. Wang, H. Huang, P. Camy, U. Griebner, V. Petrov, J.M. Serres, R.M. Solé, M. Aguiló, F. Díaz, X. Mateos. Opt. Mater., **117**, 111128 (2021). DOI: 10.1016/j.optmat.2021.111128
[14] H. Wu, G.H. Pan, Z. Hao, L. Zhang, X. Zhang, L. Zhang, H. Zhao, J. Zhang. J. Am. Ceram. Soc., **102** (8), 4919 (2019). DOI: 10.1111/jace.16325
[15] N. Zhang, Z. Wang, S. Liu, W. Jing, H. Huang, Z. Huang, K. Tian, Z. Yang, Y. Zhao, U. Griebner, V. Petrov, W. Chen. Opt. Express., **30** (13), 23978 (2022). DOI: 10.1364/OE.462701
[16] A. Pirri, R.N. Maksimov, J. Li, M. Vannini, G. Toci. Materials, **15** (6), 2084 (2022). DOI: 10.3390/ma15062084
[17] W. Jing, P. Loiko, J.M. Serres, Y. Wang, E. Kifle, E. Vilejshikova, M. Aguiló, F. Díaz, U. Griebner, H. Huang, V. Petrov, X. Mateos. J. Lumin., **203**, 145 (2018). DOI: 10.1016/j.jlumin.2018.06.043
[18] A. Schmidt, V. Petrov, U. Griebner, R. Peters, K. Petermann, G. Huber, C. Fiebig, K. Paschke, G. Erbert. Opt. Lett., **35** (4), 511 (2010). DOI: 10.1364/OL.35.000511
[19] Y. Wang, W. Jing, P. Loiko, Y. Zhao, H. Huang, X. Mateos, S. Suomalainen, A. Härkönen, M. Guina, U. Griebner, V. Petrov. Opt. Express., **26** (8), 10299 (2018). DOI: 10.1364/OE.26.010299
[20] R. Maksimov, V. Shitov, V. Osipov, O. Samatov, D. Vakalov, F. Malyavin, L. Basyrova, P. Loiko, P. Camy. Opt. Mat., **137**, 113542 (2023). DOI: 10.1016/j.optmat.2023.113542

Translated by T.Zorina